



Full paper

## 2D piezotronics in atomically thin zinc oxide sheets: Interfacing gating and channel width gating

Longfei Wang<sup>a,b,c,1</sup>, Shuhai Liu<sup>d,1</sup>, Zidong Zhang<sup>f,1</sup>, Xiaolong Feng<sup>g</sup>, Laipan Zhu<sup>a,b</sup>, Hengyu Guo<sup>a,b,c</sup>, Wenbo Ding<sup>c</sup>, Libo Chen<sup>a,b</sup>, Yong Qin<sup>d,e,\*\*</sup>, Zhong Lin Wang<sup>a,b,c,\*</sup>

<sup>a</sup> CAS Center for Excellence in Nanoscience, Beijing Key Laboratory of Micro-nano Energy and Sensor, Beijing Institute of Nanoenergy and Nanosystems, Chinese Academy of Sciences, Beijing, 100083, PR China

<sup>b</sup> School of Nanoscience and Technology, University of Chinese Academy of Sciences, Beijing 100049, PR China

<sup>c</sup> School of Material Science and Engineering, Georgia Institute of Technology, Atlanta, GA 30332, United States

<sup>d</sup> School of Advanced Materials and Nanotechnology, Xidian University, 710071, China

<sup>e</sup> Institute of Nanoscience and Nanotechnology, School of Physical Science and Technology, Lanzhou University, Gansu 730000, China

<sup>f</sup> Key Laboratory for Liquid-Solid Structural Evolution and Processing of Materials (Ministry of Education), Shandong University, Jinan 250061, China

<sup>g</sup> Microsystems and Terahertz Research Center, China Academy of Engineering Physics, Chengdu, Sichuan 610200, China

### ARTICLE INFO

#### Keywords:

Piezotronic effect  
Two-dimensional piezotronics  
Interfacing gating effect  
Channel width gating effect  
ZnO nanosheet

### ABSTRACT

Piezotronics has potential applications in human-machine interfacing, smart skin and robotics. Here, we report the first study of two-dimensional (2D) piezotronics based on atomically thin ZnO sheets. Using the inner crystal out-of-plane potential generated by the piezoelectric polarization charges created at atomically thin ZnO surfaces under stress/strain to simultaneously modulate the metal-ZnO Schottky barrier height and the conductive channel width of ZnO, the electronic transport processes in the two-terminal devices are effectively tuned by external mechanical stimuli. Moreover, the thickness dependence of 2D piezotronics is investigated to deeply explore the inner tuning mechanism. As decreasing the thickness of ZnO from tens of nanometre to atomic scale, the gauge factor is improved to  $\sim 2 \times 10^8$ . The strain sensitivity is enhanced by over three orders of magnitude owing to the increased effective piezoelectric polarizations, which is in contrast to the conventional field effect transistor with the reduce of channel lengths. This study presents in-depth understandings about the 2D piezotronics in both interfacing gating and channel width gating in piezotronics, which fundamentally paves a way for applying 2D materials with out-of-plane piezoelectricity and semiconducting property in next generation of electromechanical nanodevices.

### 1. Introduction

The adaptive and seamless interactions between electronics and physical environment are crucial for human-machine interfacing, smart skin and robotics, which demand the detection, processing and control of information encoded from environmental stimuli by functional nanodevices [1,2]. Mechanical triggering signals such as vibration and biological movements are ubiquitous and abundant in environment, which can power and control the nanodevices [3,4]. It is, however, not easy to directly interact mechanical stimuli with current electronic technologies without innovative designs or approaches. The most conventional approach is to use sensors that are sensitive to mechanical

stimuli [5–8]. The signals from sensors can be detected and recorded by conventional electronics, but they cannot be utilized to further control electronics, which is the so-called *passive* electronics. Therefore, innovative technologies are urgently needed to intelligently combine the mechanical stimulation with electronic design for human-machine interfacing.

The coupling of piezoelectricity and electronic transport processes in piezoelectric semiconductor materials under mechanical stimuli results in an emerging field of piezotronics [9–12]. When a strain/stress is induced in a piezoelectric semiconductor, the piezoelectric polarization charges created at metal-semiconductor interface can effectively modulate the Schottky barrier height (SBH) by exerting substantial

\* Corresponding author. CAS Center for Excellence in Nanoscience, Beijing Key Laboratory of Micro-nano Energy and Sensor, Beijing Institute of Nanoenergy and Nanosystems, Chinese Academy of Sciences, Beijing, 100083, PR China.

\*\* Corresponding author. School of Advanced Materials and Nanotechnology, Xidian University, 710071, China.

E-mail addresses: [qinyong@xidian.edu.cn](mailto:qinyong@xidian.edu.cn) (Y. Qin), [zhong.wang@mse.gatech.edu](mailto:zhong.wang@mse.gatech.edu) (Z.L. Wang).

<sup>1</sup> These authors contributed equally to this work.

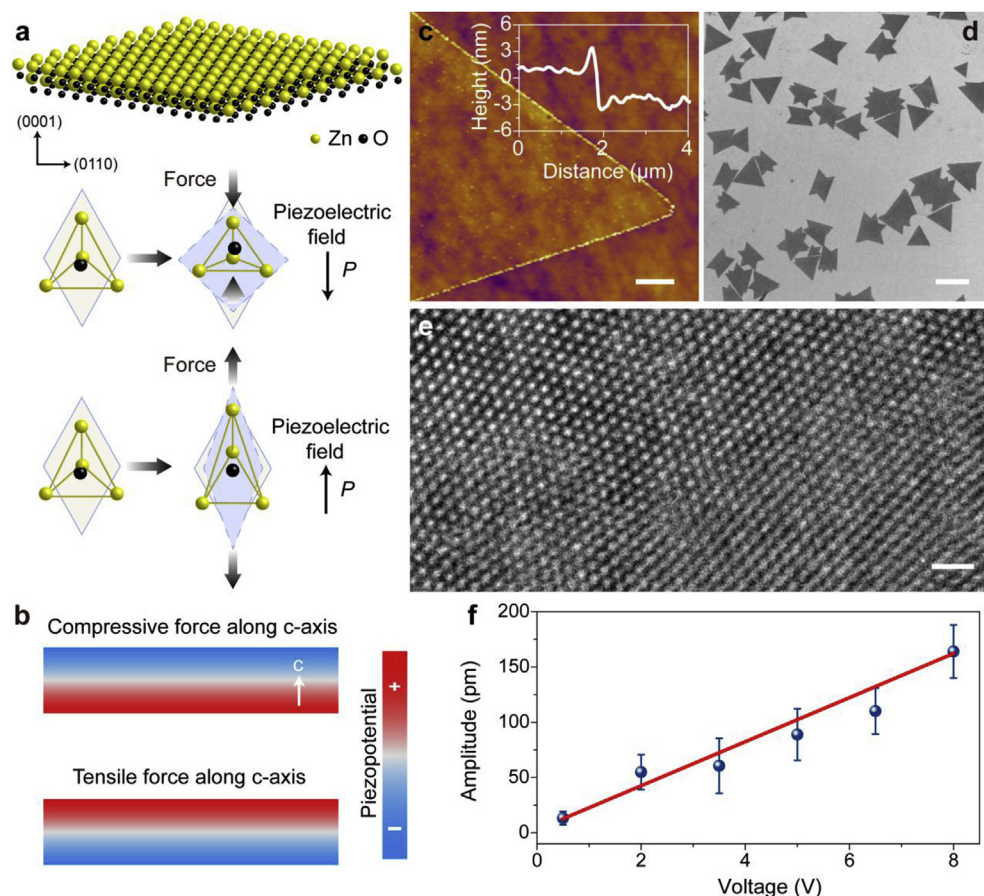


**Fig. 1.** Solution-grown atomically thin ZnO sheets and material characterization. **a**, Atomically thin ZnO sheets with a hexagonal structure consist of Zn–O–Zn stacking with the O atom centered in the tetrahedron. A piezoelectric field points towards the  $-c/c$ -axis when the unit cell of ZnO nanosheet is compressed/stretched by external force along the  $c$ -axis. **b**, Finite element analysis result of the piezoelectric polarization distribution in ZnO nanosheet under stresses. The piezoelectric polarization induced in ZnO nanosheet is positive in the red color region and negative in the blue region. **c**, Atomic force microscopy (AFM) topography of a typical ZnO nanosheet. Scale bar, 1  $\mu\text{m}$ . **d**, Scanning electron microscope (SEM) of a typical ZnO nanosheet. Scale bar, 50  $\mu\text{m}$ . **e**, HRTEM image of the ZnO nanosheet reveals the single-crystalline nature. Scale bar, 1 nm. **f**, Average piezoelectric response amplitude as a function of applied voltages extracted from statistical distribution of amplitude variations of ZnO nanosheet and substrate. Error bars indicate standard deviation. The linearly fitted line shows that the measured piezoelectric coefficient  $d_{\text{eff}}$ .

influences on the concentration and distribution of free carriers at the interface, so as to control the transport process of charge carriers. The magnitude and polarity of the piezoelectric polarization charges induced piezopotential within a piezotronic device depend on the crystallographic orientation of the piezoelectric semiconductor and the polarity of the applied local stress/strain. This is the piezotronic effect, which has been demonstrated in wurtzite structured semiconductors, such as ZnO, GaN and CdS [3,14–19]. Using inner crystal potential generated by the piezoelectric polarization charges as a ‘gate’ controlling signal to modulate the interfacing barrier and achieve tunable electronic processes is the piezotronics. It can be used to design intelligent electronic devices for directly generating digital signals to control electronics using mechanical actions without the need for external gate electrode or any other patterning processes that are challenging at a few nanometre scale lengths, which is considered as the *active* electronics. However, the currently reported piezotronic devices are mainly made of one-dimensional (1D) micro/nanowires with the sizes in the order of micrometers [3,13–19].

The exploration of 2D materials with piezoelectricity and semiconducting property has been a focus of research recently due to their promising properties of high crystallinity, ultrahigh strain tenability and compatibility with surface fabrication technologies [20–22]. The specific qualities offered by 2D materials may overcome the limitations caused by 1D nanostructures and could fully take advantage of the state-of-art micro/nano-fabrication technologies [20–25]. The demonstration of transition metal dichalcogenides (TMDs) based piezotronic devices demonstrated the possible applications of 2D materials in electromechanical nanodevices [26–31], but the basic working mechanism of these devices are essentially same with that of 1D micro/nanowires based piezotronic devices due to their anisotropy of in-plane piezoelectricity. 2D materials with out-of-plane piezoelectricity and semiconducting property may have great applications in

electromechanical nanodevices. Different from 1D micro/nanowire and 2D TMDs with in-plane piezoelectricity, the piezoelectric polarization charges will present at the entire surfaces of the 2D materials under axial strain/stress, which will have a huge impact on the concentration and distribution of free carriers in all regions of the films due to their atomic thickness and out-of-plane piezoelectricity. The coupling between out-of-plane piezoelectricity and semiconducting property in 2D materials may create new physical mechanism and broaden the piezotronic effect. However, piezotronics in this kind of 2D materials has not been explored to date.

Here, we report 2D piezotronics based on atomically thin ZnO sheets for the first time. The electronic transport processes in the two-terminal devices are effectively tuned by external mechanical stimuli, which arises from the joint modulation of two effect: the interfacing gating effect, in which stress-induced piezoelectric polarization charges at metal–ZnO interfaces modulate the SBH, and the channel width gating effect, in which stress-induced piezoelectric polarization charges at the top and bottom surfaces of ZnO control the conductive channel width. Using inner crystal out-of-plane potential generated by the piezoelectric polarization charges in 2D materials as a ‘gate’ controlling signal to simultaneously modulate the interfacing barrier and the conductive channel width, and thus to achieve tunable electronic processes is the 2D piezotronics. In addition, the thickness dependence of 2D piezotronics is investigated to deeply explore the inner tuning mechanism. As the thickness of ZnO decreases from tens of nanometre to atomic scale, the gauge factor is improved to  $\sim 2 \times 10^8$ . The strain sensitivity is enhanced by over three orders of magnitude owing to the increased effective piezoelectric polarizations resulted from the reduced carrier screening effect. This study shows the effectiveness of ‘gating’ effect of the piezoelectric polarization charges in the atomically thin ZnO sheets, presents in-depth understandings about the 2D piezotronics, and paves a way of 2D materials with out-of-plane

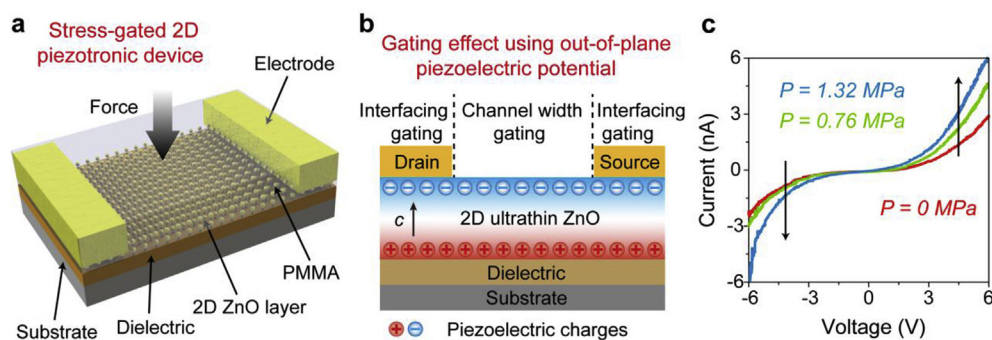


**Fig. 2.** Stress gated 2D ZnO piezotronic devices and the working mechanism. a, Schematic illustration of the 2D ZnO piezotronic device. b, Physical mechanism of the 2D piezotronics: Gating effect of stress-induced piezoelectric polarization charges at entire surfaces of atomically thin ZnO sheet. c, The modulation of carrier transport in the 2D piezotronic device under compressive stresses.

piezoelectricity and semiconducting property for applications in next generation of electromechanical nanodevices.

## 2. Results

### 2.1. Characterizations of atomically thin ZnO sheets

The ZnO nanosheets are prepared by water-air method with the *c*-axis perpendicular to the liquid level [32,33]. Atomic force microscopy (AFM) is carried out to determine the surface morphology and thickness of the obtained nanosheet. The thickness of the ZnO nanosheet is found to be approximately 2–3 nm (Fig. 1c). A typical morphology of the as-synthesized ZnO nanosheet is a single triangle with edges from ~10 to 40  $\mu\text{m}$  (Fig. 1d). High-resolution transmission electron microscopy (HRTEM) image reveals single-crystalline nature of the nanosheet (Fig. 1e). Corresponding fast Fourier transfer pattern of the HRTEM image further confirms the single crystallinity and the six-fold symmetry of ZnO nanosheet (Fig. S1). In the water-air growth method, oleylsulfate monolayers used as a soft template to guide the growth of ZnO nanosheet are inevitably transferred along with the atomically thin sheets. Considering the only few nanometre thickness, the surface adsorbed molecules may have profound influence on the electrical properties of ZnO nanosheets. The electronic property of the ZnO nanosheet is investigated by fabricating field effect transistors (Fig. S2). The  $I_d$ - $V_g$  curve shows an increasing source-drain current as the gate voltage scans from positive to negative, which is a typical p-type semiconductor behavior and has been demonstrated in previous works [32,33].

### 2.2. Out-of-plane piezoelectric property of atomically thin ZnO sheets

Based on the detailed characterization, the hexagonal structure of ZnO nanosheet still preserves even when its thickness decreases to a few atomic layers (Fig. 1a and Fig. S1), which ensures that the crystal with non-centrosymmetry structure still has piezoelectricity along the *c*-axis direction. The centers of the cations and the anions are relatively displaced when the unit cell is compressed/stretched by external force, resulting in a piezoelectric polarization, which is the origin of the piezoelectricity along *c*-axis. Finite element analysis is carried out to theoretically verify the distribution of piezoelectric polarization in the strained atomically thin ZnO sheet. The result suggests that the piezopotential is distributed along the thickness direction with opposite polarities when reversed forces along the *c*-axis direction are applied (Fig. 1b). The fundamental piezoelectric characteristics of the synthesized ZnO nanosheets are investigated by piezoresponse force microscopy (PFM), the most widely and extensively used technique to characterize nano-scale piezoelectricity [34–36]. During the PFM measurements, tip's voltages from 0.5 to 8.0 V are applied to characterize the vertical piezoresponse of the atomically thin sheet. The amplitude images and phase images under different driving voltages are shown in Fig. S3 and Fig. S4. It is observed that the piezoresponse increases steadily with higher driving voltage, indicating a strong inverse piezoelectric effect. The insets represent the statistical distributions of

amplitude variations of the ZnO nanosheet and the substrate. Piezoresponse amplitudes of ZnO nanosheet versus applied voltages are calculated from the entire areas in Fig. S3 and the calculation method is detailed in Fig. S5. From the plot of piezoresponse amplitude as a function of the applied voltage, the effective piezoelectric coefficient ( $d_{\text{eff}}$ ) of ZnO nanosheet is quantitatively calculated to be  $\sim 21.5 \pm 1.5 \text{ pm}\cdot\text{V}^{-1}$  (Fig. 1f), which is approximately two times larger than that of the bulk ZnO crystal and also outperforms many of the previous reported 2D materials (Table S1) [37–40]. The improvement in the value of  $d_{\text{eff}}$  is presumable due to the low carrier concentration and the changes in local polarization, which results from low dimensional structure with large surface, defect and charge redistribution near the surfaces [36,41]. The strong out-of-plane piezoelectricity of ZnO nanosheet makes it an ideal candidate for ultrathin electromechanical devices.

### 2.3. Piezotronic effect in 2D piezotronic devices based on atomically thin ZnO sheets

We characterized the electrical transport properties of the 2D electronic devices under compressive stress at room temperature. The two-terminal devices fabricated with metal-semiconductor-metal (M-S-M) structure are packaged by polymethyl methacrylate (PMMA) (Fig. 2a). In this configuration, the stress-induced opposite piezoelectric polarization charges present at the entire surfaces of the ZnO nanosheet, which will have a huge influence on the concentration and distribution of free carriers in all regions of the 2D film due to its atomic thickness. For the 2D piezotronic device, the current increases steadily with the increase of compressive stress (Fig. 2c). The changes in the electrical transport arise from the joint modulation of two effects: the interfacing gating effect [9–12], in which stress-induced piezoelectric polarization charges at metal-ZnO interfaces modulate the Schottky barriers, and the channel width gating effect, in which stress-induced piezoelectric polarization charges at the top and bottom surfaces of ZnO control the conductive channel width (Fig. 2b). Distinct from the previous reports of 1D micro/nanowires and 2D TMDs based piezotronic devices [3,13–19,27–31], of which the electrical transport process is mainly controlled by the interfacing gating effect, the physical mechanism of piezotronic effect in the atomically thin ZnO sheet based piezotronic devices is extended to the joint modulation of interfacing gating and channel width gating, resulting from the atomic thickness, out-of-plane piezoelectricity, and semiconducting property of the nanosheet. Using inner crystal out-of-plane potential generated by the piezoelectric polarization charges generated in 2D materials as a ‘gate’ controlling signal to simultaneously modulate the interface barrier and the conductive channel width, and thus to achieve tunable electronic processes is the 2D piezotronics. The controllable modulation of interface Schottky contacts and channel width in 2D electronic devices by stress-induced out-of-plane piezopotential may offer an approach that is unavailable to conventional technologies using external electrical control signals for tunable electronics.

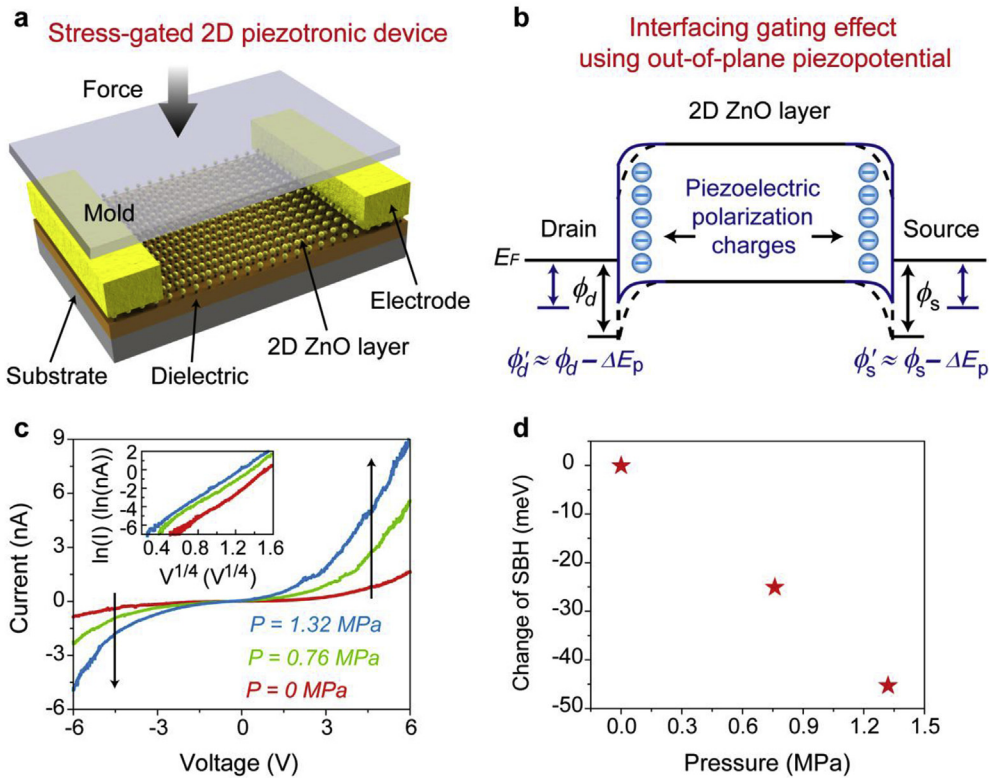


**Fig. 3.** Interfacing gating effect in 2D ZnO piezotronic device. a, Schematic illustration of 2D ZnO piezotronic device. b, Band diagrams explain the piezotronic behavior as a result of the changes in Schottky barrier heights by negative piezoelectric polarization charges.  $\phi_d$ ,  $\phi_s$  represent the Schottky barrier heights formed at drain and source contacts.  $\Delta E_p$  indicates the change of Schottky barrier height by piezoelectric polarization charges. c, Symmetric modulation of carrier transport by stresses on the metal-ZnO contacts in the piezotronic devices shows characteristics of interfacing gating effect. d, Calculated SBH change as a function of the applied pressures.

#### 2.4. Interfacing gating effect in 2D piezotronic devices

To elaborate the interfacing gating effect, we fabricate the 2D electronic devices based on atomically thin ZnO with M-S-M structure, which consists of two back-to-back Schottky barriers, and the forces are only applied on the electrodes (Fig. 3a). In this configuration, the stress-induced piezoelectric polarization charges only exist at metal-ZnO interfaces, which has a profound influence on the concentration and distribution of free carriers in ZnO nanosheet near the contact as well as on the distribution of electronic charges at metal-ZnO interface [9–12,42]. Generally, the negative piezoelectric polarization charges and hence the negative piezopotential can attract the holes near the interface, which can simultaneously lower both Schottky barriers of the metal-ZnO contacts and hence significantly increase the transport conductance (Fig. 3b). Conversely, the positive piezoelectric polarization charges and hence the positive piezopotential can repel the holes towards the interface, which can simultaneously increase the Schottky barriers and hence significantly decrease the transport conductance (Fig. S6). The magnitude and polarity of the piezopotential depend on the crystallographic orientation of the ZnO nanosheet and the direction of the applied stress. Therefore, the carrier transport process across the Schottky barrier is controlled effectively by the stress-induced out-of-plane piezopotential.

The electrical transport properties of the 2D piezotronic devices under compressive pressures are characterized (Fig. 3c). The current dramatically increases as the pressure increased, which indicates that the Schottky barrier gradually decreased with the increased pressures. To better understand the regulation mechanism, we adopt the classic Schottky theory to derive the change of SBH from the  $I_{ds}-V_{ds}$  curves [15,43,44]. According to the Schottky theory,  $\ln(I)$  is approximately proportional to  $V$  or  $V^{1/4}$ , corresponding to the thermionic-field-emission (TFE) and thermionic-emission-diffusion (TED) models. By plotting both  $\ln(I)-V^{1/4}$  and  $\ln(I)-V$  curves, we determined that the  $\ln(I)-V^{1/4}$  is almost linear (Fig. 3c, inset), which indicates that the dominant process in our experiment is TED and there exists a mirror force at the Schottky junction and the barrier is not that ‘sharp’. In addition, the

change of SBH is calculated, which shows an approximately linear relationship with applied pressures, demonstrating that the stress-induced out-of-plane piezopotential can effectively modulate the SBH (Fig. 3d). Consequently, the transport of carriers across the metal-ZnO Schottky contacts can be effectively modulated by the out-of-plane piezopotential, which can be controlled by varying the magnitude of the externally applied stress.

#### 2.5. Channel width gating effect in 2D piezotronic devices

In order to evaluate the channel width gating effect, the atomically thin ZnO sheet based piezotronic devices with M-S-M structure are fabricated with external forces applied on the channel (Fig. 4a). In this configuration, the stress-induced opposite piezoelectric polarization charges will only present at the surfaces of ZnO nanosheet in the channel region, which has a huge influence on the concentration and distribution of free carriers along the c-axis direction of ZnO nanosheet [9–12,42]. When axial compressive stress is applied on ZnO nanosheet, the positive piezoelectric polarization charges repel the holes and the negative piezoelectric polarization charges attract the holes along c-axis direction, resulting in the formation of a depletion region at the bottom of ZnO nanosheet. This depletion region will dramatically increase the channel resistance of ZnO nanosheet and thus decrease the transport conductance (Fig. 4b). In contrast, when the ZnO nanosheet is under axial tensile stress, a reversed piezoelectric field will be induced owing to its crystallographic orientation, the repelled holes are accumulated at the bottom of the ZnO nanosheet and the depletion region is formed at the top (Fig. S7), which will give rise to the same change in the channel resistance of ZnO nanosheet as well. In practice, the mobile holes in ZnO nanosheet may have resulted in partial screening of the stress-induced negative piezoelectric polarization charges and hence could affect the width of the depletion region [45], but it is still possible to observe the tunable transport characteristics. The spatial distribution of hole concentrations along the c-axis direction under a series of compressive strains is theoretically calculated via finite element analysis (Fig. 4c), which further confirms the influence of the stress-induced

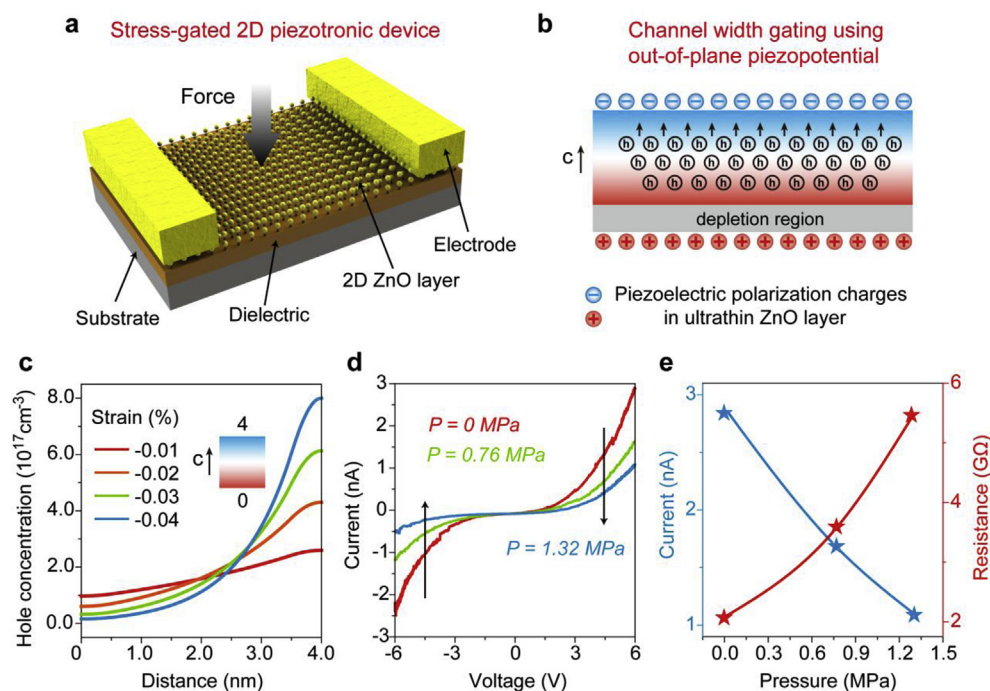


**Fig. 4.** Channel width gating effect in 2D ZnO piezotronic device. **a**, Schematic illustration of 2D ZnO piezotronic device. **b**, Schematic illustration of hole redistribution under compressive stress and the formation of depletion region in ZnO nanosheet. **c**, Spatial distribution of local hole concentration along the *c*-axis within ZnO nanosheet under different compressive strain conditions. **d**, The symmetric modulation of carrier transport by stresses on the channel in the piezotronic devices shows the characteristics of channel width gating effect. **e**, Current and corresponding conductive channel resistance with different stresses at a bias of 6.0 V.

piezoelectric polarization charges on the concentration and distribution of free carriers in ZnO nanosheet.

The electrical transport properties of the 2D electronic devices under compressive stress are characterized (Fig. 4d). The current gradually decreases as the stress increases, whereas the opposite trend of channel resistance is observed (Fig. 4e). This symmetric modulation is consistent with the above physical mechanism analysis, further demonstrating that the stress-induced out-of-plane piezopotential can effectively modulate the conductive channel width. Therefore, the mechanical stress can function as a controlling gate signal to tune the transport properties of 2D piezotronic devices by forming a depletion region to shrink the conducting channel and thus increase the resistance of the ZnO nanosheet. This working mechanism is fundamentally new in physics, which is innovative in a way that the traditional channel width gating using external gate voltage replaced by inner out-of-plane piezopotential, with the possibility of breaking the scaling limit of the conventional field effect transistor. This effect is universal and widely exists in 2D materials with out-of-plane piezoelectricity and semi-conducting property.

## 2.6. Thickness dependence of interfacial gating effect

To in-depth understand the physical mechanism of the 2D piezotronics and provide guidance to their potential applications in high-performance electromechanical devices, the thickness dependence of interfacial gating effect and channel width gating effect are investigated via finite element analysis.

Interfacial gating effect in ZnO with various thicknesses is studied by applying a series of mechanical strains on the 2D piezotronic devices with ideal back-to-back Schottky barriers. The electrical transport characteristics of the devices based on ZnO with different thicknesses are shown in Fig. 5a and Fig. S8. Obviously, the output currents with distinguishable magnitudes increase under the enlargement of compressive strains at each thickness conditions. The corresponding changes of SBH for different ZnO thicknesses, related to the out-of-plane piezopotential in controlling carrier transport across interfaces of metal-ZnO, can be derived from  $I_{\text{ds}}-V_{\text{ds}}$  plots (Fig. 5b). As the thickness of ZnO decreases, the changes of SBH become more and more significant. Fig. 5c intuitively reveals the negative correlation between the

change of SBH and the thickness of ZnO. In order to quantitatively characterize the thickness dependence of interfacial gating effect, a strain sensitivity is defined as the relative changes of SBH per unit strain:  $\Delta \text{SBH}(\epsilon)/\Delta \epsilon = [\text{SBH}(\epsilon) - \text{SBH}(\epsilon_0)]/\epsilon$ , where  $\Delta \text{SBH}(\epsilon)$  and  $\Delta \text{SBH}(\epsilon_0)$  correspond to the changes of SBH under the strain  $\epsilon$  and strain-free conditions, respectively. The strain sensitivity is improved from  $900 \pm 5.83 \text{ meV}$  for the 100 nm-thick ZnO to  $1331.77 \pm 8.53 \text{ meV}$  for the 2 nm-thick ZnO, which is extensively enhanced by  $\sim 149\%$ .

Furthermore, the physical mechanism of the thickness dependence of interfacial gating effect is carefully studied. Under compressive strains, the negative piezoelectric polarization charges are induced at metal-ZnO interfaces, which can effectively lower both Schottky barriers of the ZnO-metal contacts. However, at equilibrium state, most of the negative piezoelectric polarization charges at the interfaces are screened by mobile holes in p-type ZnO [9–12,42,45]. Hence, the holes concentration in the ZnO nanosheet is critical to the interfacial gating effect. The spatial distribution of holes concentration along the direction of metal-ZnO contact showing in Fig. 5d under strain-free condition is theoretically calculated via finite element analysis (Fig. 5e). It can be seen that the holes concentration decreases rapidly along the ZnO-metal direction and the width of depletion region reaches about 100 nm. Moreover, as the thickness of ZnO down to a few nanometre (especially within 10 nm), most of the holes are depleted. Therefore, the carrier screening effect with thinner ZnO is significantly reduced due to the low holes concentration. Energy band diagrams of ZnO with various thicknesses along *c*-axis are schematically presented to further explain the thickness dependence of interfacial gating effect in 2D piezotronic devices (Fig. 5f). Two points should be noted here. First, the energy band diagrams may cross the width of ZnO due to the width of depletion region. Second, under strain-free condition, the SBHs of the contact between metal and ZnO with various thicknesses are the same, because it depends only on the work function of metal and ZnO. By applying compressive strains along the *c*-axis, with the thickness decreasing from 100 nm to 2 nm, the effective negative piezoelectric polarization charges induced at the metal-ZnO contact are increased significantly owing to the reduced carrier screening effect. Therefore, the Schottky barrier is modulated more effectively by the negative piezoelectric polarization charges and the interfacial gating effect is dramatically enhanced when the thickness of ZnO is reduced to atomic

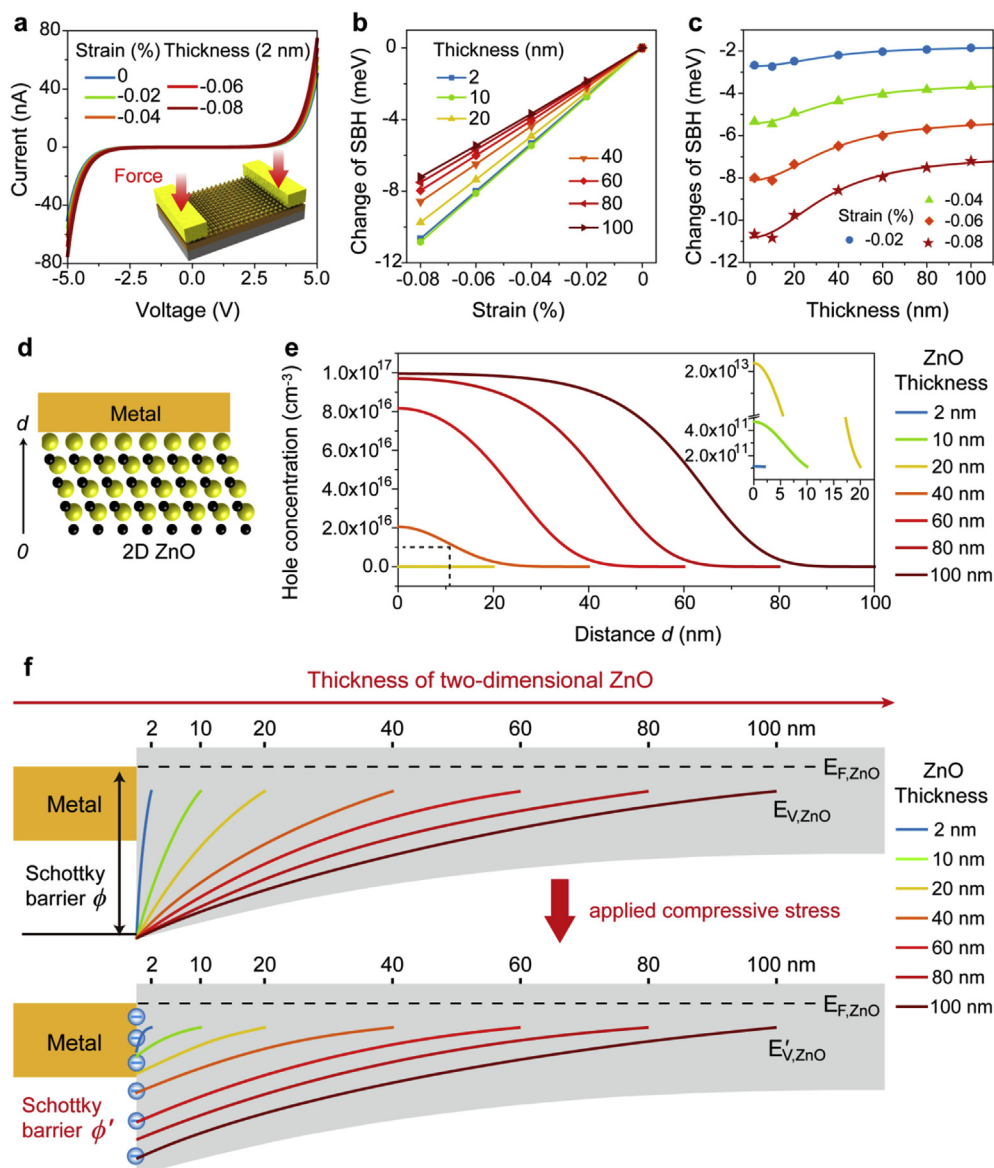


**Fig. 5.** Thickness dependence of interfacing gating effect in 2D ZnO piezotronic devices. a, Theoretically calculated  $I_{ds}$ - $V_{ds}$  characteristics of 2D ZnO piezotronic devices under a series of compressive strains on the electrodes. Inset: schematic illustration of 2D ZnO piezotronic device. b, c, Schottky barrier height change at local contact with different ZnO thicknesses as a function of compressive strains, which shows that the strain sensitivity of the piezotronic devices decreases with the thickness of ZnO increasing. e, Spatial distribution of local hole concentration within ZnO nanosheet along the direction showing in d under strain free condition. The inset is an enlargement of the dotted frame area. The acceptor concentration is  $N_A = 1 \cdot 10^{17} \text{cm}^{-3}$ . f, Band diagrams explain the thickness dependence of interfacing gating effect as a result of the different degrees of variation in the height of Schottky barrier by negative piezoelectric polarization charges.  $\phi$  and  $\phi'$  represent the Schottky barrier heights before and after applied strains, respectively.

scale.

### 2.7. Thickness dependence of channel width gating effect

The electrical transport of 2D piezotronic devices based on ZnO with various thicknesses is characterized by applied a series of compressive strains on the channel to explored the thickness dependence of channel-width gating effect (Fig. 6a and Fig. S9). The 2D piezotronic devices are designed with Ohmic contact to eliminate the influence of interface barrier on the current output. The results clearly show that, the output currents of 2D piezotronic devices are suppressed under larger compressive strains and gradually change into diode-like behavior. The mechanical strain can effectively gate the carrier transport of the piezotronic devices based on ZnO with various thicknesses, but with distinguishable magnitudes. The normalized current under compressive strains in Fig. 6b intuitively reveals that the thinner the ZnO is, the more significant the current changes will be, indicating that the channel width gating effect become more effective as the thickness of ZnO decreases. To quantitatively characterize the thickness dependence of channel width gating effect, a gauge factor is defined as the relative changes of output currents per unit strain:  $|dI/I_0 \Delta \epsilon| = (I_{\epsilon} - I_0) / (-\epsilon I_0)$ , where  $I_{\epsilon}$  and  $I_{\epsilon=0}$  correspond to the output currents under the strain  $\epsilon$

and strain-free conditions, respectively. The corresponding gauge factors are calculated at different thicknesses of ZnO and strain conditions as plotted in Fig. S10, which demonstrates that the strain sensitivity is remarkably improved with the thicknesses of ZnO decreased. The gauge factor reaches  $\sim 2 \times 10^8$ , which is enhanced by over three orders of magnitude as the thickness of ZnO decreases from 40 to 2 nm.

Besides, the physical mechanism of the thickness dependence of channel width gating effect is investigated intensively. When axial compressive stress is applied on ZnO, the positive piezoelectric polarization charges induced at bottom surface of ZnO repel the holes and the negative piezoelectric polarization charges induced at top surface of ZnO attract the holes along c-axis direction, resulting in the formation of a depletion region at the bottom of ZnO, which can significantly increase the effective channel resistance of ZnO and hence decrease the transport conductance. However, at equilibrium state, most of the negative piezoelectric polarization charges are screened by mobile holes [9–12,42,45], which results a weakened channel width gating effect. Under strain-free condition, the current output of piezotronic devices based on the thicker ZnO is much larger, which indicates that the number and the mobility of holes are much higher in the thicker ZnO. Hence, the carrier screening effect within the thicker ZnO is more significant. The channels of ZnO with various thicknesses along in-plane

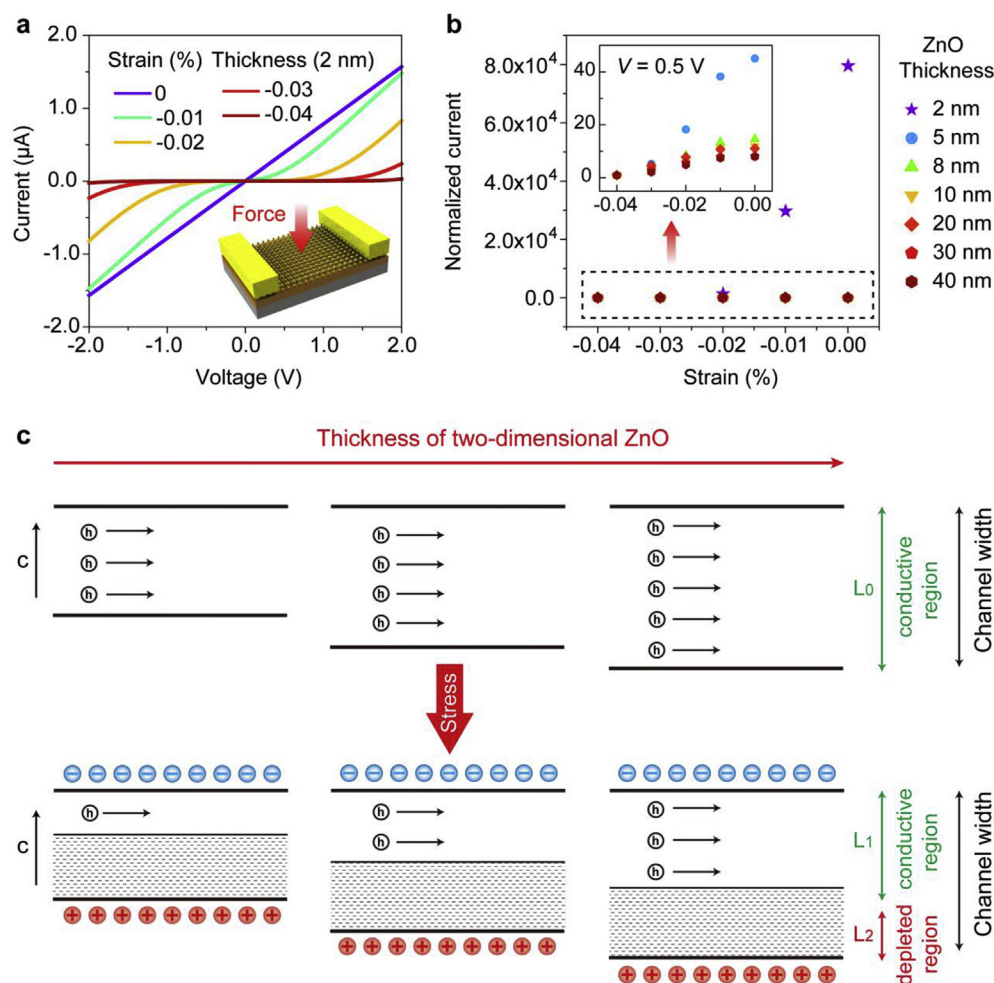


**Fig. 6.** Thickness dependence of channel width gating effect in 2D ZnO piezotronic devices. **a**, Theoretically calculated  $I_{ds}$ - $V_{ds}$  characteristics of 2D ZnO piezotronic devices under a series of compressive strains on the channel. Inset: schematic illustration of 2D ZnO piezotronic device. **b**, Normalized current change of the piezotronic devices with different ZnO thicknesses as a function of compressive strains, indicating that the strain sensitivity of piezotronic devices decreases as the thickness of ZnO increases. The inset is an enlargement of the dotted frame area. **c**, Schematic illustrations explain the thickness dependence of channel width gating effect as a result of the different degrees of variation in the width of effective depleted region and effective conductive region by the piezoelectric polarization charges.

are schematically presented in Fig. 6c to vividly explain the physical mechanism of the thickness dependence of channel width gating effect. Under compressive strains along the *c*-axis, with the thickness increasing, the effective depletion region  $L_2/L_0$  is decreased and the effective conductive region  $L_1/L_0$  is gradually increased owing to the increased carrier screening effect, where the  $L_2$  is the width of the depletion region under strain, the  $L_1$  and  $L_0$  are the width of the conductive region under strain and strain free conditions, respectively. Therefore, the channel width is gated more effectively by the piezoelectric polarization charges and the channel width gating effect is dramatically enhanced as the thickness of ZnO down to atomic scale.

### 3. Discussion

In summary, the 2D piezotronics in atomically thin ZnO sheets is explored for the first time. The electronic transport processes of the 2D piezotronic devices are effectively modulated by external mechanical stimuli, which arises from the joint modulation of two effects: the interfacial gating effect, in which the stress-induced piezoelectric polarization charges at metal-ZnO interfaces modulate the SBH, and the channel width gating effect, in which the stress-induced piezoelectric polarization charges at the top and bottom surfaces of ZnO control the conductive channel width. This is the 2D piezotronics, which is universal and widely exists in 2D materials with out-of-plane piezoelectricity and semiconducting property. Furthermore, the thickness dependence of the 2D piezotronics in both interfacial gating and channel width gating is investigated to deeply explore the inner tuning mechanism. As decreasing the thickness of ZnO from tens of nanometre to atomic scale, the gauge factor is improved to  $\sim 2 \times 10^8$ , which is

enhanced by over three orders of magnitude owing to the increased effective piezoelectric polarizations. This study shows the effectiveness of ‘gating’ effect of the piezoelectric polarization charges in the atomically thin ZnO sheets, presents in-depth understandings about the 2D piezotronics and paves a way of 2D materials with out-of-plane piezoelectricity and semiconducting property for applications in next generation of electromechanical nanodevices such as human-machine interfacing, smart skin and robotics.

## 4. Methods

### 4.1. Synthesis of atomically thin ZnO sheets

We synthesized ZnO nanosheets by using water-air method. In a typical preparation of ZnO nanosheet, 17 mL aqueous solution containing 25 mM  $Zn(NO_3)_2$  and hexamethylenetetramine (HMT) were prepared in a glass vial. Subsequently, 10  $\mu$ L chloroform solution containing 0.1 vol% sodium oleyl sulfate was spread on the solution surface. The glass vial was placed in a 60 °C convection oven. A single layer of ZnO nanosheets would appear in about 100 min and covered the water-air interface, which could be scooped using an arbitrary substrate for characterization and device fabrication.

### 4.2. Characterisations of atomically thin ZnO sheets

For Atomic force microscopy (AFM), Scanning electron microscope (SEM) characterizations, ZnO nanosheets were transferred to  $SiO_2/Si$  substrates. The morphology and thickness of the ZnO nanosheets were characterized by using AFM tapping mode (MFP-3D™, Asylum

Research). The force constant of Si tips is 2.8 N/m, and the resonance frequency is  $\sim 75$  kHz. A HITACHI S-8020 field-emission scanning electron microscope (FE-SEM) was also used to characterize the morphology of the ZnO nanosheets. For Transmission electron microscopy (TEM) characterization, ZnO nanosheets were transferred to Quantifoil holey carbon TEM grids using direct transfer method. TEM analysis was performed by using a FEI TECNAI F20 microscope.

#### 4.3. Piezoresponse force microscopy (PFM) investigates the out-of-plane piezoelectricity of ZnO nanosheet

The out-of-plane piezoelectricity of ZnO nanosheets was performed using AFM (MFP-3D™, Asylum Research) with PFM mode. The conductive tips of Pt/Ir coating, with the force constant of 2.8 N/m, were used in PFM mode. The resonance frequency is  $\sim 380$  kHz for PFM mode. The tip's voltages from 0.5 to 8.0 V were applied to study the vertical electro-mechanical response of ZnO nanosheet. In order to accurately calculate the deformation of ZnO nanosheet under different voltages, we count the amplitude values of ZnO and substrate from entire areas. Then the average amplitude variations of ZnO versus applied voltages can be calculated by subtracting the amplitude values of the substrate. All samples were examined in a sealed chamber under ambient laboratory conditions.

#### 4.4. Fabrication of field effect transistors (FET) and electrical measurement

Firstly, the SiO<sub>2</sub>/Si wafer substrates were cleaned by acetone, isopropyl alcohol, and deionized water, respectively. The ZnO nanosheets were transferred onto the Si wafer with 100 nm thermally grown SiO<sub>2</sub>. The devices were fabricated by standard e-beam lithography (EBL) process as follow: First, a layer of 200 nm positive e-beam photoresist (MICRO CHEM 950 PMMA A4) was spin-coated on the substrate at 4000 rpm for 60 s, and then baked at 150 °C for 5 min. Then the source/drain electrodes were subsequently defined by standard EBL, electron-beam evaporation of Cr/Au (10 nm/50 nm), and lift-off process. The electrical characterization of the devices was conducted with a semiconductor parameter analyzer (Keithley 4200) in a probe station under ambient environment.

#### 4.5. Fabrication of two-dimensional (2D) piezotronic devices and electrical measurement

The fabricated processes of 2D piezotronic devices are same with that of FET. The  $I_{ds}$ - $V_{ds}$  characteristics of the devices were measured and recorded by a customized computer-controlled measurement system with a function generator (Model No. DS345, Stanford Research Systems, Inc.) and a low-noise current preamplifier (Model No. SR570, Stanford 329 Research Systems, Inc.). The forces were applied on the piezotronic devices by using dynamometer for demonstration of piezotronic effect and interfacing gating effect in atomically thin ZnO sheets and AFM system with plateau tips (MFP-3D™, Asylum Research) for demonstration of channel width gating effect in atomically thin ZnO sheets. These kinds of tips have a spring constant of  $\sim 48.31$  nN/nm and inverse optical lever sensitivity (InvOLS) of  $\sim 150.75$  nm/V. The measurements were taken at room temperature.

#### 4.6. Theoretical calculations

The ZnO nanosheet is modeled as a simplified 2D cross section. The length is 20  $\mu$ m and the height is from 2 nm to 100 nm. The material constants for numerical simulation are the piezoelectric constant  $e_{33} = 11.52$  C m<sup>-2</sup>, the relative dielectric constant  $\epsilon_r = 8.91$ , the mobility of electrons  $\mu_n = 205$  cm<sup>2</sup>V<sup>-1</sup>S<sup>-1</sup> and holes  $\mu_p = 20$  cm<sup>2</sup>V<sup>-1</sup>S<sup>-1</sup>. Effective mass for  $m_e$  and  $m_h$  are 0.32  $m_0$  and 0.50  $m_0$  respectively. The electron affinity  $\chi$  adopted here is 4.5 eV and the band gap  $E_g$  is 3.37 eV. The temperature is  $T = 300$  K and the acceptor concentration

is  $N_A = 1.0 \cdot 10^{17}$  cm<sup>-3</sup>. The boundary conditions and strains are applied as the previous literature which has been demonstrated. Finally, these conditions are solved by stationary solvers in COMSOL Multiphysics.

#### Author contributions

Z.L.W., L.F.W., Y.Q. and S.H.L. conceived the project. Z.L.W., L.F.W., Y.Q. and S.H.L. designed the experiments. L.F.W., S.H.L. and Z.D.Z. performed the materials synthesis, characterizations and analyzed the results. L.P.Z. and L.B.C. fabricated the field effect transistors and piezotronic devices. L.F.W. and S.H.L. performed the electrical measurements of piezotronic devices and analysis. Z.D.Z. and X.L.F. performed the theoretical calculations and analysis. All authors contributed to discussions and writing of the manuscript.

#### Conflicts of interest

The authors declare no competing financial interest.

#### Acknowledgements

This research was supported by the National Key R&D Project from Minister of Science and Technology (2016YFA0202704), Beijing Municipal Science and Technology Commission (Z171100000317001, Z171100002017017, Y3993113DF), and National Natural Science Foundation of China (Grant Nos. 11704032, 51432005, 5151101243, 51561145021, 51322203 and 51472111).

#### Appendix A. Supplementary data

Supplementary data to this article can be found online at <https://doi.org/10.1016/j.nanoen.2019.03.076>.

#### References

- [1] S.A. Morin, R.F. Shepherd, S.W. Kwok, A.A. Stokes, A. Nemiroski, G.M. Whitesides, Camouflage and display for soft machines, *Science* 337 (6096) (2012) 828–832.
- [2] J.R. Tumbleston, D. Shirvanyants, N. Ermoshkin, R. Januszewicz, A.R. Johnson, D. Kelly, K. Chen, R. Pinschmidt, J.P. Rolland, A. Ermoshkin, E.T. Samulski, J.M. DeSimone, Continuous liquid interface production of 3D objects, *Science* 347 (6228) (2015) 1349–1352.
- [3] W.Z. Wu, X.N. Wen, Z.L. Wang, Taxel-addressable matrix of vertical-nanowire piezotronic transistors for active and adaptive tactile imaging, *Science* 340 (6135) (2013) 952–957.
- [4] Z.L. Wang, W.Z. Wu, Nanotechnology-enabled energy harvesting for self-powered micro-/nanosystems, *Angew. Chem. Int. Ed.* 51 (47) (2012) 11700–11721.
- [5] K. Takei, T. Takahashi, J.C. Ho, H. Ko, A.G. Gillies, P.W. Leu, R.S. Fearing, A. Javey, Nanowire active-matrix circuitry for low-voltage macroscale artificial skin, *Nat. Mater.* 9 (10) (2010) 821–826.
- [6] S.C.B. Mannsfeld, B.C.K. Tee, R.M. Stoltenberg, C. Chen, S. Barman, B.V.O. Muir, A.N. Sokolov, C. Reese, Z.N. Bao, Highly sensitive flexible pressure sensors with microstructured rubber dielectric layers, *Nat. Mater.* 9 (10) (2010) 859–864.
- [7] D.J. Lipomi, M. Vosgueritchian, B.C.K. Tee, S.L. Hellstrom, J.A. Lee, C.H. Fox, Z.N. Bao, Skin-like pressure and strain sensors based on transparent elastic films of carbon nanotubes, *Nat. Nanotechnol.* 6 (12) (2011) 788–792.
- [8] D.H. Kim, N.S. Lu, R. Ma, Y.S. Kim, R.H. Kim, S.D. Wang, J. Wu, S.M. Won, H. Tao, A. Islam, K.J. Yu, T.I. Kim, R. Chowdhury, M. Ying, L.Z. Xu, M. Li, H.J. Chung, H. Keum, M. McCormick, P. Liu, Y.W. Zhang, F.G. Omenetto, Y.G. Huang, T. Coleman, J.A. Rogers, Epidermal electronics, *Science* 333 (6044) (2011) 838–843.
- [9] Z.L. Wang, Nanopiezotronics, *Adv. Mater.* 19 (6) (2007) 889–892.
- [10] Z.L. Wang, Piezopotential gated nanowire devices: Piezotronics and piezo-phototronics, *Nano Today* 5 (6) (2010) 540–552.
- [11] Z.L. Wang, W.Z. Wu, Piezotronics and piezo-phototronics: fundamentals and applications, *Natl. Sci. Rev.* 1 (1) (2014) 62–90.
- [12] W.Z. Wu, Z.L. Wang, Piezotronics and piezo-phototronics for adaptive electronics and optoelectronics, *Nat. Rev. Mater.* 1 (7) (2016) 17.
- [13] Z.L. Wang, J.H. Song, Piezoelectric nanogenerators based on zinc oxide nanowire arrays, *Science* 312 (5771) (2006) 242–246.
- [14] W.Z. Wu, Y.G. Wei, Z.L. Wang, Strain-gated piezotronic logic nanodevices, *Adv. Mater.* 22 (42) (2010) 4711.
- [15] S.H. Liu, L.F. Wang, X.L. Feng, Z. Wang, Q. Xu, S. Bai, Y. Qin, Z.L. Wang, Ultrasensitive 2D ZnO piezotronic transistor array for high resolution tactile imaging, *Adv. Mater.* 29 (16) (2017).
- [16] L.F. Wang, S.H. Liu, X.L. Feng, Q. Xu, S. Bai, L.P. Zhu, L.B. Chen, Y. Qin, Z.L. Wang,

- Ultrasensitive vertical piezotronic transistor based on ZnO twin nanoplatelet, *ACS Nano* 11 (5) (2017) 4859–4865.
- [17] R.M. Yu, L. Dong, C.F. Pan, S.M. Niu, H.F. Liu, W. Liu, S. Chua, D.Z. Chi, Z.L. Wang, Piezotronic effect on the transport properties of GaN nanobelts for active flexible electronics, *Adv. Mater.* 24 (26) (2012) 3532–3537.
- [18] S.H. Liu, L.F. Wang, Z. Wang, Y.F. Cai, X.L. Feng, Y. Qin, Z.L. Wang, Double-channel piezotronic transistors for highly sensitive pressure sensing, *ACS Nano* 12 (2) (2018) 1732–1738.
- [19] C.F. Pan, L. Dong, G. Zhu, S.M. Niu, R.M. Yu, Q. Yang, Y. Liu, Z.L. Wang, High-resolution electroluminescent imaging of pressure distribution using a piezoelectric nanowire LED array, *Nat. Photon.* 7 (9) (2013) 752–758.
- [20] M.N. Blonsky, H.L.L. Zhuang, A.K. Singh, R.G. Hennig, Ab initio prediction of piezoelectricity in two-dimensional materials, *ACS Nano* 9 (10) (2015) 9885–9891.
- [21] K.A.N. Duerloo, M.T. Ong, E.J. Reed, Intrinsic piezoelectricity in two-dimensional materials, *J. Phys. Chem. Lett.* 3 (19) (2012) 2871–2876.
- [22] R. Hinchet, U. Khan, C. Falconi, S.W. Kim, Piezoelectric properties in two-dimensional materials: Simulations and experiments, *Mater. Today* 21 (6) (2018) 611–630.
- [23] D.E. Perea, E.R. Hemesath, E.J. Schwalbach, J.L. Lensch-Falk, P.W. Voorhees, L.J. Lauhon, Direct measurement of dopant distribution in an individual vapour-liquid-solid nanowire, *Nat. Nanotechnol.* 4 (5) (2009) 315–319.
- [24] G.H. Lee, R.C. Cooper, S.J. An, S. Lee, A. van der Zande, N. Petrone, A.G. Hammerberg, C. Lee, B. Crawford, W. Oliver, J.W. Kysar, J. Hone, High-strength chemical-vapor deposited graphene and grain boundaries, *Science* 340 (6136) (2013) 1073–1076.
- [25] C. Lee, X.D. Wei, J.W. Kysar, J. Hone, Measurement of the elastic properties and intrinsic strength of monolayer graphene, *Science* 321 (5887) (2008) 385–388.
- [26] H.Y. Zhu, Y. Wang, J. Xiao, M. Liu, S.M. Xiong, Z.J. Wong, Z.L. Ye, Y. Ye, X.B. Yin, X. Zhang, Observation of piezoelectricity in free-standing monolayer MoS<sub>2</sub>, *Nat. Nanotechnol.* 10 (2) (2015) 151–155.
- [27] W.Z. Wu, L. Wang, Y.L. Li, F. Zhang, L. Lin, S.M. Niu, D. Chenet, X. Zhang, Y.F. Hao, T.F. Heinz, J. Hone, Z.L. Wang, Piezoelectricity of single-atomic-layer MoS<sub>2</sub> for energy conversion and piezotronics, *Nature* 514 (7523) (2014) 470.
- [28] J.J. Qi, Y.W. Lan, A.Z. Stieg, J.H. Chen, Y.L. Zhong, L.J. Li, C.D. Chen, Y. Zhang, K.L. Wang, Piezoelectric effect in chemical vapour deposition-grown atomic-monolayer triangular molybdenum disulfide piezotronics, *Nat. Commun.* 6 (2015) 7430.
- [29] W.Z. Wu, L. Wang, R.M. Yu, Y.Y. Liu, S.H. Wei, J. Hone, Z.L. Wang, Piezophototronic effect in single-atomic-layer MoS<sub>2</sub> for strain-gated flexible optoelectronics, *Adv. Mater.* 28 (38) (2016) 8463–8468.
- [30] S.A. Han, T.H. Kim, S.K. Kim, K.H. Lee, H.J. Park, J.H. Lee, S.W. Kim, Point-defect-passivated MoS<sub>2</sub> nanosheet-based high performance piezoelectric nanogenerator, *Adv. Mater.* 30 (21) (2018).
- [31] J.H. Lee, J.Y. Park, E.B. Cho, T.Y. Kim, S.A. Han, T.H. Kim, Y. Liu, S.K. Kim, C.J. Roh, H.J. Yoon, H. Ryu, W. Seung, J.S. Lee, J. Lee, S.W. Kim, Reliable Piezoelectricity in bilayer WSe<sub>2</sub> for piezoelectric nanogenerators, *Adv. Mater.* 29 (29) (2017) 1606667.
- [32] F. Wang, J.H. Seo, G.F. Luo, M.B. Starr, Z.D. Li, D.L. Geng, X. Yin, S.Y. Wang, D.G. Fraser, D. Morgan, Z.Q. Ma, X.D. Wang, Nanometre-thick single-crystalline nanosheets grown at the water-air interface, *Nat. Commun.* 7 (2016) 10444.
- [33] L.F. Wang, S.H. Liu, G.Y. Gao, Y.K. Pang, X. Yin, X.L. Feng, L.P. Zhu, Y. Bai, L.B. Chen, T.X. Xiao, X.D. Wang, Y. Qin, Z.L. Wang, Ultrathin piezotronic transistors with 2 nm channel lengths, *ACS Nano* 12 (5) (2018) 4903–4908.
- [34] G.D. Rodrigues, P. Zelenovskiy, K. Romanyuk, S. Luchkin, Y. Kopelevich, A. Kholkin, Strong piezoelectricity in single-layer graphene deposited on SiO<sub>2</sub> grating substrates, *Nat. Commun.* 6 (2015) 7572.
- [35] Y.K. Yan, J.E. Zhou, D. Maurya, Y.U. Wang, S. Priya, Giant piezoelectric voltage coefficient in grain-oriented modified PbTiO<sub>3</sub> material, *Nat. Commun.* 7 (2016) 13089.
- [36] X.W. Wang, X.X. He, H.F. Zhu, L.F. Sun, W. Fu, X.L. Wang, L.C. Hoong, H. Wang, Q.S. Zeng, W. Zhao, J. Wei, Z. Jin, Z.X. Shen, J. Liu, T. Zhang, Z. Liu, Subatomic deformation driven by vertical piezoelectricity from CdS ultrathin films, *Sci. Adv.* 2 (7) (2016) e1600209.
- [37] D.F. Crisler, J.J. Cupal, A.R. Moore, Dielectric piezoelectric and electromechanical coupling constants of Zinc Oxide crystals, *Proc. IEEE* 56 (2) (1968) 225.
- [38] L. Dong, J. Lou, V.B. Shenoy, Large in-plane and vertical piezoelectricity in janus transition metal dichalcogenides, *ACS Nano* 11 (8) (2017) 8242–8248.
- [39] C.J. Brennan, R. Ghosh, K. Koul, S.K. Banerjee, N.S. Lu, E.T. Yu, Out-of-plane electromechanical response of monolayer molybdenum disulfide measured by piezoresponse force microscopy, *Nano Lett.* 17 (9) (2017) 5464–5471.
- [40] N. Syed, A. Zavabeti, J.Z. Ou, M. Mohiuddin, N. Pillai, B.J. Carey, B.Y. Zhang, R.S. Datta, A. Jannat, F. Haque, K.A. Messalea, C.L. Xu, S.P. Russo, C.F. McConville, T. Daeneke, K. Kalantar-Zadeh, Printing two-dimensional gallium phosphate out of liquid metal, *Nat. Commun.* 9 (2018) 3618.
- [41] D.A. Scrymgeour, J.W.P. Hsu, Correlated piezoelectric and electrical properties in individual ZnO nanorods, *Nano Lett.* 8 (8) (2008) 2204–2209.
- [42] Y. Zhang, Y. Liu, Z.L. Wang, Fundamental theory of piezotronics, *Adv. Mater.* 23 (27) (2011) 3004–3013.
- [43] Y.S. Zhou, R. Hinchet, Y. Yang, G. Ardila, R. Songmuang, F. Zhang, Y. Zhang, W.H. Han, K. Pradel, L. Montes, M. Mouis, Z.L. Wang, Nano-Newton transverse force sensor using a vertical GaN nanowire based on the piezotronic effect, *Adv. Mater.* 25 (6) (2013) 883–888.
- [44] W.H. Han, Y.S. Zhou, Y. Zhang, C.Y. Chen, L. Lin, X. Wang, S.H. Wang, Z.L. Wang, Strain-gated piezotronic transistors based on vertical Zinc Oxide nanowires, *ACS Nano* 6 (5) (2012) 3760–3766.
- [45] Y. Gao, Z.L. Wang, Equilibrium potential of free charge carriers in a bent

piezoelectric semiconductive nanowire, *Nano Lett.* 9 (3) (2009) 1103–1110.



**Longfei Wang** received his B.S. (2012) in Materials Science and Engineering from China University of Geosciences (Beijing) and Ph.D. (2017) in Nanoscience and Technology from Beijing Institute of Nanoenergy and Nanosystems, Chinese Academy of Sciences. He is now a postdoctoral fellow in Professor Zhong Lin Wang's group at Georgia Institute of Technology. His current research focuses on piezotronics and piezo-phototronics.



**Shuhai Liu** received his B.S. (2012) in Applied Physics from Hua Zhong University of Science and Technology and M.S. (2015) in Condensed Matter Physics from University of Chinese Academy of Sciences. From 2015 to 2017, he worked as an assistant engineer in China Electronics Technology Group Corporation. Now he is a Ph.D student in Professor Yong Qin's group at Xidian University. His research mainly focuses on piezotronics, piezo-phototronics and fundamental physical properties characterization based on atomic force microscopy.



**Zidong Zhang** received his B.S. and Ph.D. degree in Material Science and Engineering from Shandong University (2013). He worked as a visiting scholar (2012–2013) in the Institute for Superconducting and Electronic Materials (ISEM), University of Wollongong, Australia. Now he is an Associate Professor at the School of Material Science and Engineering, Shandong University, Jinan, China. His current research focuses on electromagnetic metamaterials and paper-based electronic devices for electromagnetic energy harvesting.



**Xiaolong Feng** received his M.S. degree from Beijing Institute of Nanoenergy and Nanosystems, University of Chinese Academy of Sciences. Now he is a PhD student at Singapore University of Technology and Design, in Shengyuan Yang's Research Lab for Quantum Materials. His research interests focus on topological materials and transport effect.



**Laipan Zhu** received his B.S. degree in Physics department from Shandong University in 2010 and his Ph.D. in Institute of Semiconductors, Chinese Academic of Sciences in 2015. Now he is an associate professor in Prof. Zhong Lin Wang's group in Beijing Institute of nanoenergy and nanosystems, Chinese Academic of Sciences. His main research interests have been focused on the field of piezotronics, piezo-phototronics and spintronics.



**Hengyu Guo** received his B. S. and Ph.D. degree in Applied Physics from Chongqing University, China. Now he is a postdoctoral fellow in Georgia institute of technology, Zhong Lin Wang' group. His current research interest is triboelectric nanogenerator based energy and sensor systems.



**Yong Qin** received his B.S. (1999) in Material Physics and Ph.D. (2004) in Material Physics and Chemistry from Lanzhou University. From 2007 to 2009, he worked as a visiting scholar and Postdoc in Professor Zhong Lin Wang's group at Georgia Institute of Technology. Currently, he is a professor at the Institute of Nanoscience and Nanotechnology, Lanzhou University, where he holds a Cheung Kong Chair Professorship. His research interests include nanoenergy technology, functional nanodevice and self-powered nanosystem. Details can be found at: <http://www.yqin.lzu.edu.cn>.



**Wenbo Ding** received the B.E and Ph.D. degrees (highest honors) from the Department of Electronic Engineering, Tsinghua University, Beijing, China, in 2011 and 2016, respectively. He is now a postdoctoral fellow at Georgia Tech, Atlanta, GA, working with Professor Z. L. Wang. His research interests include self-powered sensors, energy harvesting, human-machine interface with the help of signal processing and machine learning. He has received many prestigious awards, including the IEEE Scott Helt Memorial Award, the Tsinghua Top Grade Scholarship (highest honor in Tsinghua), the Excellent Ph.D. Graduate of Beijing City, and the Excellent Doctoral Dissertation of Tsinghua University.



**Zhong Lin Wang** received his Ph.D. from Arizona State University in physics. He now is the Hightower Chair in Materials Science and Engineering, Regents' Professor, Engineering Distinguished Professor and Director, Center for Nanostructure Characterization, at Georgia Tech. Dr. Wang has made original and innovative contributions to the synthesis, discovery, characterization and understanding of fundamental physical properties of oxide nanobelts and nanowires, as well as applications of nanowires in energy sciences, electronics, optoelectronics and biological science. His discovery and breakthroughs in developing nanogenerators established the principle and technological road map for harvesting mechanical energy from environment and biological systems for powering personal electronics.

His research on self-powered nanosystems has inspired the worldwide effort in academia and industry for studying energy for micro-nano-systems, which is now a distinct disciplinary in energy research and future sensor networks. He coined and pioneered the field of piezotronics and piezophotonics by introducing piezoelectric potential gated charge transport process in fabricating new electronic and optoelectronic devices. Details can be found at: <http://www.nanoscience.gatech.edu>.



**Libo Chen** received his B.S. degree in Physics from Zhengzhou University, China and Ph.D. degree in Condensed Matter Physics from University of Chinese Academy Sciences, China. Now he is a postdoctoral researcher in Uppsala University, Sweden. His current research interest is piezotronic and tribotronic devices and their application in self-powered systems.